NIH Public Access
Author Manuscript
J Pharm Sci. Author manuscript; available in PMC 2013 October 01.

Published in final edited form as:
J Pharm Sci. 2012 October ; 101(10): 3763–3778. doi:10.1002/jps.23256.

Antibody nanoparticle dispersions formed with mixtures of crowding molecules retain activity and in vivo bioavailability

Maria A. Miller, **Tarik A. Khan**, **Kevin J. Kaczorowski**, **Brian K. Wilson**, **Aileen K. Dinin**, **Ameya U. Borwankar**, **Miguel A. Rodrigues**, **Thomas M. Truskett**[*], **Keith P. Johnston**[*], and **Jennifer A. Maynard**[*]
Department of Chemical Engineering, University of Texas at Austin, Austin, TX 78712

Abstract

Monoclonal antibodies continue to command a large market for treatment of a variety of diseases. In many cases, the doses required for therapeutic efficacy are large, limiting options for antibody delivery and administration. We report a novel formulation strategy based on dispersions of antibody nanoclusters that allows for subcutaneous injection of highly concentrated antibody (~190 mg/ml). A solution of monoclonal antibody 1B7 was rapidly frozen and lyophilized using a novel spiral-wound *in situ* freezing technology (SWIFT) to generate amorphous particles. Upon gentle stirring, a translucent dispersion of ~430 nm protein clusters low apparent viscosity (~24 cp) formed rapidly in buffer containing the pharmaceutically acceptable crowding agents, trehalose, polyethylene glycol and n-methyl-2-pyrrolidone. Upon *in vitro* dilution of the dispersion, the nanoclusters rapidly reverted to monomeric protein with full activity, as monitored by dynamic light scattering and antigen binding. When administered to mice as an intravenous solution, subcutaneous solution or subcutaneous dispersion at similar (4.6-7.3 mg/kg) or ultra-high dosages (51.6 mg/kg), the distribution and elimination kinetics were within error and the protein retained full activity. Overall, this method of generating high-concentration, low-viscosity dispersions of antibody nanoclusters could lead to improved administration and patient compliance, providing new opportunities for the biotechnology industry.

Introduction

Monoclonal antibodies have generated considerable interest as therapeutics because they specifically target distinct antigens with favorable pharmacokinetic, production, and safety profiles. Currently, 29 monoclonal antibodies have received FDA approval for treatment of a wide variety of diseases, commanding an annual market size of over $20 billion dollars[1,2]. Despite advances in protein drug development which allow tailoring of key biophysical properties‘, such as solubility[3], stability[4], and binding affinity[5] via recombinant DNA techniques, few options have been developed to deliver these macromolecules at desired dosages (>2 mg antibody/ kg body weight). Typically, large volumes of dilute protein solutions are delivered intravenously to avoid the chemical and physical destabilization and resulting loss in protein activity commonly associated with high concentration formulations[6,7]. For instance, Rituxan doses of 100-500 mg are currently administered by intravenous infusion of a 10 mg/ml solution[8]. Self-administered subcutaneous injections offer several major advantages over intravenous infusion, including increased accessibility and patient compliance, along with reduced pain and cost. However, the required therapeutic

[*]To whom all correspondence should be addressed, The University of Texas at Austin, Department of Chemical Engineering, 1 University Station CO400, Austin, TX, 78712. JAM: (512) 471-9188 (phone), (512)471-7060 (fax), maynard@che.utexas.edu; KPJ: (512) 471-4617 (phone), (512)471-7060 (fax), kpj@che.utexas.edu; TMT: (512) 471-6308 (phone), (512)471-7060 (fax), ttruskett@utexas.edu. .

NIH-PA Author Manuscript
NIH-PA Author Manuscript
NIH-PA Author Manuscript

NIH-PA Author Manuscript

NIH-PA Author Manuscript

NIH-PA Author Manuscript

dosages indicate protein concentrations in excess of 100 mg/ml, given the maximum subcutaneous injection volume of 1.5 ml[9,10].

Formulation of therapeutic proteins at these high concentrations is intrinsically difficult, demanding solutions customized for each new product. Frequently, it is not possible due to low protein solubility[3,11], protein instability[12-14] and high solution viscosity[7,15,16] resulting from short-range attractive protein-protein interactions. These interactions, which include hydrophobic interactions, hydrogen bonds and fluctuating charge dipoles[16], act over distances up to ~1 nm[17]. At high protein concentrations (over 150 mg/ml), the average separation distance between individual antibody molecules is reduced to less than 10 nm[18]. Thus, the probability that two protein molecules will be less than 1 nm apart is high and the effect of the short-range attractive interactions between protein molecules becomes significant[18]. This leads to concentration-dependent formation of reversible and irreversible aggregates with potential adverse effects on protein activity, pharmacokinetics and immunogenicity. Most troubling are irreversible aggregates, high molecular weight aggregates comprised of monomers with altered structure and reduced activity, which can lead to a turbid solution or even protein precipitation. The formation of these aggregates is protein specific[19] and can form through physical mechanisms, such as partially unfolded monomers with exposed hydrophobic residues[20] or chemical mechanisms, such as formation of intermolecular bonds mediated by reactive thiols on cysteine or methionine residues[21].

Protein structure and activity in low viscosity formulations can be preserved at high protein concentrations by minimizing the effects of these short-range interactions. For example, concentrated suspensions of protein microparticles in water-insoluble organic solvents[22] and aqueous suspensions of protein crystals[7] with low viscosity have been reported. These formulations succeed by using micron-sized (5-20 μm) particles of proteins as opposed to protein monomers, thus increasing the average distance between protein particles for a given protein concentration. However, formulations of proteins in organic solvents are not desirable as they require large-bore needles and can result in inflammation at the injection site[23]. In addition, while highly concentrated aqueous suspensions of crystalline insulin have a history of clinical use[23], it is challenging to routinely crystallize large protein molecules such as immunoglobulins due to their high molecular weight, surface oligosaccharides, and segmental flexibility[7,24]. Similarly, controlled release formulations in which proteins are encapsulated in polymeric matrices with non-aqueous[25] or aqueous media[26-29] have also been explored. In these cases, the low levels of protein within the particle (~15-20 mass%) result in a low deliverable dose even at high particle volume fractions[30]. Moreover, most polymeric delivery systems suffer from challenges related to sterility, protein stability, incomplete protein release, and increased immunogenicity[31-33].

We recently reported a novel approach to preserve protein activity at high concentrations with low viscosity, via concentrated dispersions of nanoclusters, readily reversible particles (30-500 nm) composed of amorphous antibody molecules[18]. In that work, lyophilized monoclonal murine or polyclonal sheep antibody was resuspended in buffer containing trehalose as a “crowder” molecule that occupies a large volume and increases the short-range protein-protein attractive interactions.[18] Consequently, most of the protein molecules are concentrated into densely packed equilibrium nanoclusters, ~80-300 nm in diameter, depending on the trehalose concentration used.[18] A possible mechanism of nanocluster formation and stabilization was explained in terms of specific short-ranged attraction, van der Waals and depletion attraction forces balanced against weak electrostatic repulsion to result in a colloidally stable protein nanocluster dispersion of discrete size and low viscosity[18]. This hierarchy of attractive and repulsive interactions provides one possible explanation for the colloidally stable protein nanocluster dispersions with low viscosity that were observed experimentally.[18] In addition, it was hypothesized that the high volume

NIH-PA Author Manuscript

NIH-PA Author Manuscript

NIH-PA Author Manuscript

fraction of protein within the nanoclusters, much higher than is possible with a uniform protein solution, helped to maintain the native protein structure due to a self-crowding, entropic stabilizing mechanism.[34,35] Remarkably, nanocluster formation did not detectably alter the structure, antigen binding activity or *in vivo* pharmacokinetics of a monoclonal antibody.

While promising, formation of therapeutic protein nanoclusters has only been reported using standard bulk freezing prior to lyophilization followed by resuspension in dispersion buffer with a single extrinisic crowder, trehalose[18]. It is unclear whether a single extrinisic crowder will be sufficient to optimize protein formulations for the desired therapeutic properties for wide classes of proteins with varying stabilities, solubilities and molecular shapes. Additionally, more sophisticated freezing techniques than standard lyophilization may be required to preserve protein activity and engineer nanocluster particle morphology. In this study, we demonstrate that a multicomponent mixture of three crowding agents can be used to create stable dispersions of highly concentrated, active monoclonal antibody particles that retain high activity and bioavailability upon subcutaneous administration in mice.

The murine IgG2a monoclonal antibody 1B7, which binds and neutralizes the pertussis toxin (PTx) associated with whooping cough infection[36,37], was selected to demonstrate applicability to a therapeutically relevant molecule and allow comparisons with previously described trehalose-only dispersion formulations. First, amorphous protein particles were generated via a new freezing method, spiral-wound in-situ freezing technique (SWIFT). Next, these particles were dispersed in the presence of three pharmaceutically acceptable crowding agents [38]: water-soluble organic n-methyl-2-pyrrolidone (NMP), polyethylene glycol (PEG), and trehalose to yield a formulation with low viscosity (<50 cP), high antibody concentration (~200 mg/ml) and ~430 nm 1B7 nanoparticles. Importantly, the native 1B7 protein activity was preserved, as measured by *in vitro* biochemical methods and pharmacokinetics unaltered. Dispersions are a promising approach to generate highly concentrated, low viscosity antibody formulations. They can achieve dosages at least 10-fold higher than can be attained via solutions and can be formulated with a variety of pharmaceutically acceptable agents.

Experimental

Antibody expression and, purification

Murine hybridoma cells producing the IgG2a antibody 1B7 were grown in 1 liter shaker flasks in Hybridoma-SFM serum-free media (Gibco) at 37°C with 5% CO_2, as reported previously[18,37]. Briefly, antibody purification consisted of media clarification by centrifugation at 3,000 rpm for 20 minutes, followed by filter sterilization using a 0.2 μm filter, 1:1 dilution with binding buffer (20 mM pH 7.0 sodium phosphate) and loading onto a pre-equilibrated Protein-A column with an Akta FPLC system (GE Healthcare). After baseline stabilization, 1B7 was eluted into collection tubes containing 1 M Tris pH 8.0 using a low-pH elution buffer (0.1M glycine pH 2.7), concentrated and buffer exchanged with centrifugal micro-dialysis units (Centricon). Protein concentration was measured with micro-bicinchonoinic acid (BCA) assay (Pierce, Rockford, IL), while non-reducing SDS-PAGE verified protein preparation homogeneity and purity. Purified 1B7 was labeled with biotin using EZ-link® Sulfo-NHS-LC-Biotin (Pierce, Rockford, IL) to provide an orthogonal detection handle to track the murine antibody in murine serum samples. A 5 mM solution of the biotin reagent was added at a 5:1 molar ratio to a 1 mg/ml solution of the 1B7 in PBS at room temperature and allowed to react for 30 minutes. Excess biotin was removed by buffer exchange using 50,000 MWCO Centricon concentrators with PBS. Protein was >95% pure, as judged by SDS-PAGE, SEC and isoelectric focusing gel.

NIH-PA Author Manuscript

NIH-PA Author Manuscript

NIH-PA Author Manuscript

Amorphous particle formation by spiral wound in-situ freezing technology (SWIFT)

Purified and biotinylated 1B7 was buffer exchanged into 20mM pH 5.5 histidine buffer using Centricons, as above. The protein concentration was measured, solid α-α trehalose (JT Baker) was added to a 1:1 wt ratio as a cryoprotectant and gently mixed to dissolve. The resulting solution was filter sterilized (0.22 μm), diluted to 20 mg/ml protein and transferred to a sterile 8ml (1.9 cm × 4.8 cm) glass vial for SWIFT freezing. During SWIFT, the base of the vial was contacted with liquid nitrogen while rotating the vial on its side (~1 revolution/second), resulting in a thin film of frozen solution on the inside edge of the vial, with subsequent thin films freezing in a spiral towards the center of the vial (Figure 1A). After the entire volume was frozen (~10-40 seconds), the samples were placed upright on a pre-cooled lyophilizer shelf at −40°C. The samples were then lyophilized for 12 hours at −40°C at 100mTorr, followed by a 6 hour ramp to 25°C at 50 mTorr, and maintained for secondary drying at 25°C at 50 mTorr for at least an additional 6 hours. To assess protein activity after freezing, powder was reconstituted at 5 mg/ml in PBS for analysis by dynamic light scattering (DLS) and enzyme-linked immunosorbent assay (ELISA) as described below. Samples of the dry powders after lyophilization for scanning electron microscopy (SEM) analysis were placed on adhesive carbon tape to fix the sample to the SEM stub. Each sample for SEM was platinum-palladium sputter coated using a Cressington 208 bench top sputter coater to a thickness of 10nm. Micrographs were taken using a Zeiss Supra 40 VP scanning electron microscope with an accelerating voltage of 5 kV. Further characterization of particles formed by SWIFT freezing is found in the supplemental material.

Dispersion formation

To form the dispersion, SWIFT frozen and lyophilized 1B7 protein powder was compacted into 0.1ml conical vials (Wheaton Science Products No. 986211) such that the total powder weight was 0.04 ± 0.001g. An aqueous-based solvent dispersion buffer, containing 10% (v/v) PEG300 (Spectrum Chemical Manufacturing) and 20% (v/v) n-methyl-2-pyrrolidone (NMP; Malinckrodt) in a 50mM phosphate buffer with the pH adjusted to match the measured antibody pI (pH 7.2, data not shown), was added to the lyophilized protein. Gentle stirring with the tip of a needle removed air pockets, to yield a uniform, optically clear dispersion with a final 1B7 concentration of 190 mg/ml. Neither sonication nor violent mixing was necessary to form a uniform translucent dispersion. All analyses were performed within two hours of dispersion formulation.

Viscosity measurement

The apparent viscosity of the 1B7 dispersion was measured as the time to draw 50 μl of the dispersion into a 25 gauge 1.5″ long needle attached to a 1ml tuberculin slip tip syringe, as reported previously for sheep IgG dispersions[18]. Briefly, videos of the conical vial containing the dispersion were taken and the time to draw from a height 0.4″ from the bottom of the cone to a height 0.1″ from the bottom of the cone was measured using Image J software. A standard curve using known solutions with various viscosities provided a linear correlation between the time to draw 50 μl from the conical vial to the viscosity with an r^2 value greater than 0.99[18]. These results are consistent with previous work with suspensions of model proteins and protein solutions which found that the time to draw up a specified amount of the sample in a syringe was correlated linearly to viscosity[15,18,22].

Colloidal size determination/ characterization

Dynamic light scattering (DLS) was used to measure the sizes of particles present in the purified 1B7 preparation, concentrated 1B7 dispersion and dilutions of the dispersion using a custom-built DLS apparatus[39] modified to include backscattering angles up to 165°[18]. Particle sizes in the concentrated dispersion were measured with a small volume cell (60 μl,

NIH-PA Author Manuscript

NIH-PA Author Manuscript

NIH-PA Author Manuscript

Beckman Coulter #A54094) at ~23°C and a 160° scattering angle, while all other measurements were made in a standard 1 ml cell at ~23°C and scattering angles optimized to detect the relevant particle size, as analyzed with CONTIN. To estimate the concentration below which only 1B7 monomers are presentin the dispersion buffer, the 190 mg/ml dispersion was diluted 1:40, 1:80 and 1:160 in dispersion buffer and particle sizes measured at a 90° scattering angle. We define the concentration of 1B7 at which the protein monomer peak is observed by DLS as the threshold concentration for cluster formation. To mimic the effects of dilution on particle size and detect formation of aggregates, the dispersion was diluted 1:40 in PBS to give a final 5 mg/ml 1B7 concentration and the resulting particle sizes measured at a scattering angle of 30°. The size of purified 1B7 monomeric antibody in PBS was measured at 5 mg/ml and a scattering angle of 30°.

In vitro antibody activity and aggregation assays

All assays of protein activity and structural stability were conducted on 1B7 dispersion diluted to 1 mg/ml in PBS. Controls included lyophilized 1B7 and purified, untreated 1B7, both adjusted to 1 mg/ml in PBS. The formation of insoluble and di-sulfide linked aggregates was monitored by non-reducing SDS-PAGE. Here, 3 μg 1B7 sample was combined with loading buffer, separated on a 4-20% precast linear gradient polyacrylamide gel (Bio-Rad) and stained with Gel-Code Blue (Bio-Rad).

To monitor ligand-binding activity, an indirect PTx ELISA was employed as reported previously[18,37]. High-binding ELISA plates (Costar) were coated with pertussis toxin (PTx, List Biological Laboratories) at 0.75 μg/ml in PBS and incubated at 4 °C overnight. Wells were blocked with assay buffer (PBS-1% milk) for 1 hour, prior to addition of 1B7 samples in a √10 serial dilution scheme from 50 μg/ml in assay buffer. After a one hour incubation at room temperature and triplicate washes with PBS-0.05% Tween-20, goat anti-mouse IgG-horseradish peroxidase conjugate (1:2,000 dilution in assay buffer, Sigma) was incubated for one hour at room temperature. Plates were washed in triplicate and signal developed with tetramethylbenzidine dihydrochloride (TMB) substrate (Pierce), quenched with 1N HCl and the resulting absorbance at 450 nm recorded using a SpectraMax M5 instrument. The EC_{50} value was calculated from the linear range of the dose-response curve as the antibody concentration corresponding to 50% of the maximum absorbance, based on a four parameter fit. For comparison between samples, the relative EC_{50} was calculated as the ratio of the sample EC_{50} to unprocessed control antibody EC_{50}. All samples were run in triplicate.

In vivo bioavailability in BALB/c mice

An *in vivo* pharmacokinetic study of the 1B7 dispersion and control solution was performed over a 14 day period using four to six healthy 24-27g, female BALB/c mice per group. Mice were administered a single 1 or 100 μl subcutaneous injection of 1B7 at standard (4.6-7.3 mg 1B7/kg body weight) or high (~51.6 mg/kg) doses. The five sample groups compared in this study included two solution control groups receiving ***(1)*** IV and ***(2)*** subcutaneous injections of 100 μl 1B7 solution (1.4 mg/ml solution for a final 5.6 mg/kg dose)[18], as well as three test groups, receiving subcutaneous injections of ***(3)*** 100 μl of a diluted PEG-NMP dispersion at standard dose (4.6 mg/kg), ***(4)*** 1 μl dispersion at a standard (7.3 mg/kg) dose; and ***(5)*** 100 μl of dispersion at high dose (51.6 mg/kg) (see Table 2). The previously reported solution controls (groups 1 and 2) were prepared from a 20 mg/ml 1B7 solution in PBS diluted to 1.4 mg/ml in PBS[18] while the dispersion samples were diluted from a 190 mg/ml 1B7 dispersion to a concentration of 1.2 mg/ml for group 3 (at this concentration, below the threshold for nanocluster formation, the antibodies are recovered as monomers), 12.9 mg/ml for group 4, and 190 mg/ml for group 5 with dispersion buffer immediately prior to injection.

NIH-PA Author Manuscript

NIH-PA Author Manuscript

NIH-PA Author Manuscript

Prior to the injection and at eight additional timepoints between 12 and 336 hours, mice were weighed and a blood sample (~20 μl) collected from the tail vein. After collection, the samples were allowed to clot, centrifuged at 5000 rpm for 10 minutes and serum transferred to a new tube. At the terminal timepoint (336 hours), mice were anaesthetized and between 0.2 and 1 ml serum collected by cardiac puncture. These samples were used in ELISA assays, to measure the total and active concentrations of 1B7 in the serum and, for the terminal time point, to measure antibody activity via an *in vitro* neutralization assays and to provide an initial estimate of mouse anti-1B7 responses. This study was performed with approval by the Institutional Animal Care and Use Committee at the University of Texas at Austin (protocol #AUP-2010-00070) in compliance with guidelines from the Office of Laboratory Animal Welfare. To estimate t_{max} and C_{max}, a curve was fit to the pharmacokinetic data for each mouse using natural cubic spline interpolation over the entire time interval. The corresponding maximum was then determined analytically from the resulting cubic polynomial on the interval of interest. To calculate the AUC values, the data were fit to a four-parameter bi-exponential model with one termed weighted by time: $c = A \exp(-\alpha t) + B \exp(-\beta t)$. The AUC was defined as the improper integral of this model as time approaches infinity.

Measurement of 1B7 in serum samples

To determine the concentration of active 1B7 in serum samples, a standard ELISA approach was used with the following modifications as previously reported[18,40]. ELISA plates were coated with PTx at 1.5 μg/ml in PBS. The assay buffer used as diluent in all steps consists of 4% bovine serum albumin, 4% fetal bovine serum (FBS), 0.05% Tween 20, in PBS, pH 7.4. After blocking with assay buffer, 2.3 μl serum sample was serially 1:√10 diluted in 50 μl per well assay buffer. Each plate included mouse serum (Sigma) as a negative control and a 1B7 standard curve diluted to an initial concentration of 100 μg/ml in mouse serum. Additional samples were analyzed to assess total 1B7 protein levels using a streptavidin coating on the ELISA plates to detect the biotinylated 1B7.

After measurement of the resulting absorbance values, SoftMax Pro v5 was used to calculate EC_{50} values based on the serum dilution using a 4-parameter logistic (4PL) model for each individual curve. Concentrations of active 1B7 in each serum sample were calculated from a linear correlation between the log [(sample EC_{50})/ (standard EC_{50})] versus the log of the known 1B7 concentration in the standard curve. A linear correlation with a fit > 0.95 from at least 5 independent standard curves were determined.

Measurement of active antibody by CHO cell neutralization assay

As an orthogonal activity measurement to determine the concentration of serum 1B7 able to neutralize PTx activity *in vitro*, we employed a CHO cell neutralization assay modified from Gillenius *et al.*[37,41] The concentration of neutralizing antibody was measured as the sera dilution that completely inhibited PTx-induced CHO cell clustering relative to a standard curve of purified 1B7 with known concentration. Briefly, 50 μl of 0.5 ng/ml pertussis in Dulbecco's Modified Eagle Medium (DMEM) with 10% FBS was added directly to each well of a sterile 96 well tissue culture plate. Terminal serum samples (23 μl) were serially diluted into the PTx media using a 1:√10 dilution scheme. After incubation for 30 minutes at 37°C and 5% carbon dioxide, 100 μl / well of freshly trypsinized CHO cells at 10^5cells/ ml were seeded in each well. After 48 h of incubation at 37°C and 5% CO_2, wells were scored for CHO clustering using 0-3 scale, with 0 as elongated (non-clustered) and 3 as completely clustered. A 5-parameter logistic model was used to fit the assay scores against 1B7 concentration and to find the hypothetical concentration yielding a CHO score of 1.5. The molar ratio of 1B7 to PTx at this point was then calculated relative to that of the standard and reported as the relative activity.

NIH-PA Author Manuscript

NIH-PA Author Manuscript

NIH-PA Author Manuscript

Results and Discussion

Here, we report formation of highly concentrated, low viscosity dispersions of antibody nanoclusters, in which the antibody retains native size and binding activity upon dilution and *in vivo* sub-cutaneous administration. In contrast to our prior work[18], we used a novel freezing technique to form amorphous particles and multiple crowding agents to tune particle size. The combination of these innovations allowed us to administer subcutaneous antibody dispersions to mice at typical therapeutic doses (5.6-7.3 mg/kg) as well as an ultra-high dose, more than 10-fold higher than current practice (51.6 mg/kg). The measured pharmacokinetic parameters were similar for solution and dispersion formulations and antibody present in serum at the terminal timepoint retained antigen binding and neutralizing activities expected for 1B7.

Stable Protein Particles made by SWIFT freezing

The first step in preparation of concentrated aqueous dispersions is formation of a dried powder of protein particles. The choice of freezing method can be critical to both protect antibody structure and activity during freezing, as well as to produce particles of the appropriate size and morphology to yield a colloidally stable dispersion. To address these concerns, we developed a novel freezing technique, SWIFT, which rapidly freezes an antibody solution directly in the final packaging vial prior to lyophilization (see Figure 1A). The rationale in developing this technique is that two major sources of protein denaturation during freezing are exposure to liquid-gas interfaces during spray-freeze drying and the slow rate of freezing in larger volumes which can result in freeze concentration and subsequent concentration-dependent aggregation[42,43]. By rotating the vial of protein solution while in contact with liquid nitrogen, each concentric layer freezes in less than a second. The remaining liquid is gently mixed due to rotation, normalizing any concentration gradients.

We used SWIFT followed by lyophilization to form micron-sized particles of the 1B7 antibody used in the dispersions. These small particles may aid in minimizing any gel formation during the resuspension process that would adversely affect antibody activity and formulation viscosity versus tray lyophilization, which is also compatible with dispersion formulations[18]. To prevent protein aggregation during freezing, the protein solution was adjusted to contain a 1:1 weight ratio of trehalose as a cryoprotectant.[42] The buffer selected, 20 mM histidine pH 5.5, is commonly used during lyophilization steps[44]. An SEM analysis of the frozen and lyophilized 1B7 indicates the presence of micron-sized particles (Figure 1B). Importantly, antibody processed in this manner retained native size and activity upon reconstitution with PBS at 5 mg/ml. At this concentration, DLS detected a single species with a ~10nm hydrodynamic diameter, as expected for an antibody monomer[13] (Figure 2A). The absence of larger particles indicated that the antibody did not form irreversible aggregates during SWIFT and lyophilization. In addition, an ELISA to monitor the specific PTx-binding activity of the reconstituted antibody revealed no significant change in activity due to SWIFT versus the untreated control (Table 1; Figure 3A), whereas ELISA after heat treatment (70 C for 60 minutes with 1 mM DTT) did detect a significant activity loss (data not shown).

The SWIFT process was designed to protect protein structure and activity. This is achieved via rapid freezing with minimal liquid-air interface, goals inspired by related process, thin film freezing (TFF)[45]. In SWIFT, each film layer, corresponding to a single vial revolution, is ~200nm thick (see supplemental results), Indirect contact with liquid nitrogen as a heat sink confers cooling rates of ~10^2 K/s. In TFF, a small volume of protein solution is deposited on a cryogenically cooled surface, where it spreads to ~210 nm thickness, freezing within a single second[45]. Scaling-up to compare freezing times for equal volumes, TFF

NIH-PA Author Manuscript

NIH-PA Author Manuscript

NIH-PA Author Manuscript

freezes at a rate of ~5.1 seconds per ml of protein solution, while SWIFT results in a similar rate, ~7.5 seconds/ml (supplemental Figure S1).

As a result of the similarities in freezing rates and film thicknesses, TFF and SWIFT processing of similar protein solutions yields dry particles with similar morphologies (Figure 1B).[45] For TFF, and by extension, SWIFT, the rapid cooling and freezing rates generate a large number of ice nuclei, which exclude solute molecules due to freezing point depression effects. The remaining liquid is present in thin channels between ice nuclei, becomes supersaturated with dissolved crowder molecules and protein. The rapid freezing and consequent rapid vitrification of these liquid channels inhibits solute diffusion; as these molecules precipitate, the reduced collision frequency inhibits coagulation of these small insoluble particles to generate larger particles. In addition, as the concentrations of dissolved solutes rise in the unfrozen liquid, the associated viscosity increase further reduces the mobility of the growing particle nuclei. During the dehydration step, water present in these channels is removed, leaving small particles of dry protein and crowder. In contrast, traditional tray freezing lyophilization with its slower freezing rate yields larger liquid channels and larger final particles after drying.[45] Thus smaller submicron protein particles, as shown in Figure 1B, are formed during SWIFT freezing versus standard tray freezing lyophilization.

With both SWIFT and traditional tray lyophilization, low levels of protein denaturation and aggregation are achieved by kinetic and thermodynamic stabilization of the native protein structure during freezing and lyophilization. The native protein state is stabilized during lyophilization by kinetically trapping protein molecules in an amorphous solid[21,46,47], thereby reducing protein mobility that can lead to aggregation. Addition of the lyoprotectant trehalose during lyophilization further thermodynamically stabilizes the protein native state during freezing by entropically favoring the native folded state[21,46,48] and during dehydration by forming hydrogen bonds with proteins.[49,50] However, processes to rapidly freeze proteins such as spray freeze drying (SFD), have been shown to increase protein aggregation versus standard tray freezing lyophilization due to the large gas-liquid interface in the spraying step.[51,52] The large area/volume of the gas-liquid interface of ~6000 cm^{-1} in SFD for 10 μm sprayed droplets can lead to protein adsorption at the interface, denaturation and aggregation.[47,51,53-55] In the case of SWIFT, the gas-liquid interface is minimized as the only exposure of the liquid protein solution to the air is the liquid interface inside the glass vial. As a result, the estimated gas-liquid interface decreases 3 orders of magnitude when compared to SFD to ~4 cm^{-1}. Thus 1B7 was anticipated and found to remain activity upon reconstitution to monomer from the dry powder form after SWIFT freezing and lyophilization.

One practical advantage of SWIFT freezing is the ability to freeze directly in the final dosage vial when compared to other rapid freezing techniques such as TFF and SFD.[45,55,56] This approach avoids the need for costly, solid transfer steps while maintaining aseptic conditions. In this case, if a dosage of 80 mg of the protein is required at a concentration of 20 mg/ml, the 8 ml vial used in the study can serve as both the freezing and reconstitution vial. However, since the cooling rate of SWIFT freezing is governed by the liquid cryogen used and the thickness of the glass vial, as well as the heat transfer coefficients of the materials used, the vial can be readily scaled-up or down to meet dosage requirements. In addition, by removing the transfer step to the final vial, all of the protein can be recovered after lyophilization and utilized in the formation of the final dosage.

Colloidal Characterization of 1B7 particles in dispersion

To form the colloidally stable, translucent nanocluster dispersion, the dry, sub-micron particles of antibody and trehalose produced via SWIFT were combined (Figure 4A) with a

NIH-PA Author Manuscript

NIH-PA Author Manuscript

NIH-PA Author Manuscript

50 mM phosphate buffer adjusted to the antibody pI (pH 7.2) containing two additional crowding agents: 20% n-methyl-2-pyrrolidone (NMP) and 10% polyethylene glycol 300 (PEG300) by volume. After combining the SWIFT particles and dispersion buffer, the trehalose contained in the dry powder dissolves. A fraction of the trehalose will diffuse into the solution, increasing the volume fraction of crowding agents as observed previously for sheep IgG[18]. Sufficient dispersion buffer was added to the dry powder to yield a final antibody concentration of 190 mg/ml with a final 0.34 volume fraction (φ) of crowding agents.

Under these conditions, DLS with CONTIN analysis of the dispersion using a low volume (60 μL) cell identified a single population of particles with a ~432 +/− 16 nm diameter. This colloid size was reproduced in three separate experiments, measured each time in triplicate, with a representative curve shown in Figure 2B. This particle size was further confirmed by SEM images of the dispersion after dilution to 100 mg/ml in the dispersion buffer, rapid freezing and lyophilization onto an SEM stage (Figure 4B). This image shows nanoparticles of a size consistent with DLS measurements, but a different shape due to coating with crystallized trehalose. Previously, SEM and STEM images of dispersed sheep IgG and 1B7 particles at lower trehalose concentrations, visualized the dispersed particles as clusters of smaller particles[18]. We were able to obtain similar images for the current formulation after adding dispersion buffer to reduce the trehalose concentration, simultaneously reducing the 1B7 concentration to 40 mg/ml (Figure 4C). To confirm that these results are not affected by dissociation of the 1B7 nanoparticles, we determined the conditions where 1B7 nanoclusters dissociate to monomer in dispersion buffer, using methods reported previously[18]. Starting with the 190 mg/ml dispersion, we progressively added dispersion buffer to reduce the protein concentration and measured the resulting particle sizes by DLS (Figure 2B). We observed a single peak at ~430 nm until the protein concentration was reduced to 2.5 mg/ml or less. At this concentration, only a single ~10nm peak at is present, corresponding to the hydrodynamic diameter of a single monoclonal antibody molecule.[13] From these data, we conclude that 1B7 nanoclusters in this dispersion buffercompletely dissociate to monomer at ~2.5 mg/ml and that 1B7 nanoparticles formed with trehalose, PEG and NMP are fully reversible (Table 1).

The dispersed particles were formed and exhibited colloidal stability, possibly due to a previously proposed balancing of the intermolecular attractive and repulsive interactions at the protein molecular and colloidal levels, respectively[18]. Briefly, individual protein molecules are subject to highly attractive depletion and specific short-ranged interactions such as hydrophobic interactions, hydrogen bonding and charge-dipole interactions.[57,5818]. Near the 1B7 pI, longer-range electrostatic repulsion is relatively weak and thus the attraction force dominates between isolated pairs of protein molecules. However, once these molecules assemble into nanoclusters of sufficient size, the cumulative electrostatic interactions between particles in the cluster balance the attractions, stabilizing the dominant size[18]. Between clusters, short-range attractive interactions are expected to be negligible relative to electrostatic repulsion resulting in a colloidally-stable dispersion of protein nanoclusters, as has been discussed previously[18].

The strength of depletion-attraction forces can be tuned by varying the concentrations of the crowding agents[59,60]. As observed here and previously[18], an increase in crowder concentrations favors 1B7 nanocluster formation.. While 1B7 and the sheep IgG dispersions could both be formulated with a single crowding agent, trehalose, the ternary crowder system used here may provide additional flexibility to formulate dispersions with highly soluble proteins or to further control the nanocluster size, protein stability, dispersion viscosity and nanocluster degradation during delivery.

NIH-PA Author Manuscript

NIH-PA Author Manuscript

NIH-PA Author Manuscript

The low apparent viscosity, 24 cP, of the 190 mg/ml 1B7 dispersion was measured as the viscosity through a 25 gauge 1.5 inch needle (Table 1). This viscosity measurement was previously characterized for subcutaneous injections of highly concentrated solutions of monoclonal antibodies[15] and non-aqueous suspensions of lyosyzme[22]. Due to our very small sample volumes (~100 ul), we were concerned that evaporation would rapidly affect values measured with a traditional viscometer. The apparent dispersion viscosity is commonly described as a function of the intrinsic viscosity, [η], maximum volume fraction of particles, ϕ_{max}, and the solvent viscosity, η_0, using the Krieger-Dougherty equation (Eq. 1)[22,61].

$$\frac{\eta}{\eta_o}=\left[1-\left(\frac{\phi}{\phi_{\max}}\right)\right]^{-[\eta]\phi_{\max}} \quad \text{Eq. 1}$$

The η may be reduced by lowering $\eta_{0,}$ or [η], which has a minimum of 2.5 for hard sphere colloids, and increasing ϕ_{max}. For protein molecules in solution at high concentrations, for example φ = 0.1 to 0.3, strong short-range specific attractive interactions[58,62], often produce viscosities 5 to 100 times the hard sphere value[15,63]. For monoclonal antibody solutions with concentrations of 150 mg/mL, viscosities greater than 100 cP have been attributed to reversible self-association of protein molecules, on the basis of measurements by analytical ultracentrifugation.[15,64] In contrast, the low viscosities observed in the present study for the nanocluster dispersions may be consistent with the weak interactions between the nanoclusters, as suggested previously[18].

In vitro molecular stability of 1B7 dispersion

As processing steps can adversely affect protein structure and activity, we monitored the antibody size within the dispersion and after dilution using several techniques, including DLS, non-reducing SDS-PAGE and ELISA (Table 1). After a 10-fold dilution from the 190 mg/ml dispersion into PBS, DLS measured a single species with a ~10nm hydrodynamic diameter, as expected for a single antibody monomer[13] (Figure 2A). The absence of larger particles indicates the dispersion formulation does not induce irreversible aggregates and that the antibody can readily recover its monomeric size upon dilution. This is further confirmed by non-reducing SDS-PAGE (Figure 3B), in which a single band of the expected antibody monomer size ~150 kDa is observed, indicating an absence of irreversible thiol-linked and SDS-resistant aggregates.[65] Finally, an ELISA to monitor the specific PTx-binding activity of the antibody reveals no significant change in activity due to the formation or dilution of the dispersion versus untreated control based on EC_{50} comparisons (Figure 3A; Table 1).

For antibody formulated as a dispersion to maintain therapeutic efficacy upon *in vivo* injection[66,67], the native antibody activity must be maintained through every processing and delivery step: from (1) freezing and lyophilizing the antibody solution, (2) nanocluster formation via dispersion, and (3) delivery through a syringe, to (4) nanocluster dissociation and diffusion from the injection site. While loss of protein conformational stability can result from chemical degradation as well as physical denaturation processes, physical denaturation is expected to be the larger challenge to successful development of high protein concentration formulations due to its strong dependence on protein concentration.[9,66] As discussed above, the protein powder formed by SWIFT freezing and lyophilization exhibited no detectable loss in antigen-binding activity or development of aggregates after reconstitution in buffer.

It has been speculated that the use of *in vitro* self-crowding to stabilize native protein might mimic the *in vivo* intracellular environment, in which folded proteins are stabilized by a

NIH-PA Author Manuscript

NIH-PA Author Manuscript

NIH-PA Author Manuscript

high concentration of diverse molecular crowding agents (300-400 mg/ml).[34,68] In that model, the high protein volume fraction within a nanocluster allows the protein to act as its own crowding agent, entropically favoring the lowest surface area conformation of the protein, which is typically the native state[18,34,35]. This result was originally predicted theoretically[34] but the first indirect experimental validation awaited development of dispersions[18] as protein solutions cannot achieve the high protein volume fractions (>0.15) necessary. Unfolding and irreversible aggregation of protein molecules in the nanocluster is thought to be further reduced by decreased protein mobility within the highly concentrated nanocluster versus a solution[6,69,70]. Since molecule collisions can lead to the formation of aggregates, a reduced collision frequency among protein molecules at the nanocluster-buffer interface kinetically stabilizes these molecules.[12,18,71]

The retention of protein activity and the lack of detectable aggregates upon *in vitro* dilution from the concentrated dispersion is an important indication of *in vivo* protein stability. At the high concentrations of the dispersion formulation, we speculate that the 1B7 antibody is stabilized within the nanoclusters by self-crowding, at the nanocluster boundary layer and in the aqueous phase by crowders present in the dispersion buffer[72]. Similarly, the diluted 1B7 is stable at final solution concentrations (~10 mg/ml) in PBS buffer due to the inherent stability of the immunoglobulin fold, which has evolved to persist for ~23 days in serum containing 60-85 mg/ml total protein. The most aggregation-prone step will occur at intermediate concentrations, when the protein is no longer at a sufficiently high concentration for self-crowding to inhibit partial unfolding, but high enough for transiently unfolded intermediates to aggregate via concentration-dependent aggregation. Using the Noyes-Whitney equation for high surface area to volume particles, we predicted a nanocluster dissociation time, to provide an estimate of the duration the protein spends in this intermediate concentration regime. Dilution of ~430 nm antibody nanoclusters into PBS, in which 1B7 nanocluster threshold concentration is >50 mg/ml, is expected to result in particle dissociation in less than one second.

Experimentally, dilution of 1B7 protein nanoclusters with dispersion buffer to maintain a constant crowder concentration resulted in recovery of monomeric, active protein, as measured by DLS and ELISA[18]. For a trehalose-induced polyclonal sheep IgG dispersion at a constant protein concentration, a steady decrease in nanoparticle size was achieved by diluting the crowder to weaken the attractive forces between immunoglobulin molecules[18]. At each step, the clusters were fully diluted and characterized, and found to have expected activity as measured by ELISA[18]. The protein molecules on the cluster surface are expected to be crowded by protein molecules on the cluster side and sugar molecules at the cluster-buffer interface. As protein molecules diffuse away from the cluster surface into the PBS media, they retain activity as shown by the DLS and ELISA experiments.

In vivo bioavailability of stable 1B7 from dispersions

No reliable *in vitro* models exist to mimic *in vivo* dissociation of the dispersion after subcutaneous injection. Thus, we proceeded to a mouse model to measure the pharmacokinetic parameters as well as the specific activity of *in vivo* dissolved antibody material. The five treatment groups included three control groups to allow direct pharmacokinetic comparison of low volume, high concentration and large volume, high concentration dispersion test groups. The control groups 1 and 2 received a standard antibody dose (4.6-5.6 mg/kg in 100 μl) to allow for a direct comparison of the subcutaneous dispersion injection pharmacokinetics to intravenous and sub-cutaneous delivery of an antibody solution. A third control, group 3, assessed the effect of dispersion formulation on antibody pharmacokinetics, in which the dispersion was diluted to 1.4 mg/ml with dispersion buffer, a concentration below the cluster limit and comprised of antibody monomers. Two test groups were designed to assess the combined effects of dispersion

NIH-PA Author Manuscript

NIH-PA Author Manuscript

NIH-PA Author Manuscript

concentration and delivered volume on *in vivo* dissociation rates and the resulting pharmacokinetics. In group 4, these mice received a standard dose (7.3 mg/kg) administered as a high concentration dispersion (190 mg/ml) in a small 1 μl volume. Group 5 received an ultra-high antibody dose, which can only be achieved with high concentration, low viscosity formulations such as a dispersion. These mice received a ten-fold higher dose than the other groups (51.6 mg/kg in 100 μl). For all groups, serum samples were collected from the tail vein over 14 days, with the concentrations of total and active 1B7 antibody in each sample measured by streptavidin and PTx capture ELISAs, respectively. The efficacy of antibody present at the terminal time point was also assessed using an *in vitro* activity assay, based on antibody-mediated inhibition of toxin activity.

Overall, the 1B7 pharmacokinetic profile is quite similar for all groups, with distribution and elimination kinetics all within error. The primary differences result from the injection site and injection volume, affecting the time to reach the maximum concentration (t_{max}) and the value of the maximum concentration (C_{max}/ dose). Looking first at the three control groups, delivery via subcutaneous dispersion resulted in a lower C_{max}/dose and delayed t_{max}, as compared to IV and subcutaneous delivery of solutions (Table 2; Figure 5). The group 1 control IV solution reached a maximum serum concentration at the first measured time point (12 hours), followed by a rapid decrease as the antibody is distributed throughout the tissues[18]. In comparison, the subcutaneous solution group displayed a slightly reduced C_{max}/ dose (25.5 versus 18.8 ug/ml/ mg/kg) and statistically significant delayed t_{max} (15 versus 19 hrs; $p<0.05$). While IV-administered material is instantly diluted in the blood volume, material administered subcutaneously must diffuse from the injection site through interstitial fluid to reach the lymphatic and blood vessels before distribution in the blood volume, delaying these pharmacokinetic parameters (Figure 5A).[18,73] The subcutaneous dispersion injections, groups 3 and 5, exhibit similar trends as the subcutaneous solution but with a slightly lower C_{max} and delayed t_{max} when compared to the subcutaneous solution (Figure 5B). This may reflect the effects of the dispersion buffer on antibody diffusion, as the effect is minimized with group 4, standard dose subcutaneous dispersion, which was injected as a ~1 ul volume instead of a 100 ul volume using a positive displacement microvolume syringe. For this sample, the t_{max} was similar (within error) to that of the subcutaneous solution.

Once the maximum serum concentration is attained, all groups show similar 1B7 distribution and elimination pharmacokinetics. As seen in Figure 5, these data fit a biphasic exponential profile, with α distribution and β elimination time constants that are within experimental error for all groups, based on 1B7 concentrations measured by the PTx ELISA (Table 2). The β elimination half-life was also within error for all groups when measured using a total 1B7 ELISA assay, based on streptavidin detection of the biotinylated antibody (Supplemental Table S1). The distribution phase represents passive antibody diffusion from the well-mixed blood volume into other tissues, driven by the 1B7 concentration gradient and the elevated vascular pressure, while antibody elimination rates are controlled by interactions with specific receptors such as the FcRn[73,74]. Notably, both rates will vary with antibody aggregation and misfolding. A soluble aggregate will have a larger size and consequently larger diffusion constant and slower $t_{1/2}\alpha$, while a misfolded monomer or soluble aggregate will exhibit different binding kinetics for the FcRn and a different $t_{1/2}\beta$. The similar kinetics observed for all groups indicate that the antibody delivered as a subcutaneous dispersion is able to dissociate from the nanocluster and diffuse away from the injection site while retaining an active, monomeric form, similar to our *in vitro* observation in which active 1B7 monomer is rapidly recovered upon dispersion dilution.

These experiments were performed in mice, where the large permissible injection volume per body mass (100 μl/ 25g) allows for direct comparisons between solutions and

NIH-PA Author Manuscript

NIH-PA Author Manuscript

NIH-PA Author Manuscript

dispersions formulated at the same concentration. A similar comparison is not possible in humans, as subcutaneous injections are restricted to ~1.5 ml volume. To demonstrate that dispersions can achieve dosages relevant for humans, we prepared group 4 as a scaled-down version of a human dose (Figure 5B). Here, a ~1 μl volume of highly concentrated dispersion (190 mg/ml) was administered subcutaneously, for a final 7.6 mg/kg murine dosage. Scaling-up to calculate the human dosage, in which a 190 mg/ml dispersion could be administered in a 1.5 ml volume, this is equivalent to a 4.3 mg/kg human dose, exceeding current typical dosing guidelines (2 mg/kg). To evaluate the potential for dispersions to result in less-frequent administration of ultra-high antibody dosages, which are not currently achievable with solutions, group 5 mice received a large, 100 μl injection volume of highly concentrated dispersion (190 mg/ml), for a 51.6 mg/kg dose. In spite of the large error inherent to administering a 1 ul injection of a viscous solution, this group also exhibited similar pharmacokinetics (similar t_{max}, t1/2,α, t1/2,β) and 1B7 bioavailability indicating concentration and dose-independent pharmacokinetics. Reduced absolute bioavailability of 50-100% is expected for a subcutaneous administration[73]and was observed in this study as 75.4% +/− 26.4 for the sub-cutaneous solution control. The relative bioavailability of the dispersion formulations were further reduced (66.3% +/− 27.4 for the diluted dispersion, 49.8% +/− 20.4 for the standard dose dispersion, and 71.1% +/− 26.0 for the high-dose dispersion), possibly due to incomplete cluster dissociation and/or increased lymphatic processing. This decrease in relative bioavailability is likely related to the use of crowder agents employed in this study, as previous work using only trehalose resulted in relative bioavailability within error of the solution subcutaneous.[18]

To provide an orthogonal measurement of antibody quality to complement antigen ELISA, we measured 1B7 biological activity with an *in vitro* CHO cell neutralization assay using sera from the terminal time point. Free PTx will bind cell-surface receptors, undergo receptor-mediated endocytosis and eventually ADP-ribosylation of $G_{i/o}$ coupled receptors; phenotypically, the cells lose contact inhibition and grow in a clustered morphology. Antibody-mediated neutralization of PTx blocks toxin entry into cells, protecting the normal growth phenotype. Sera were diluted in the presence of a fixed PTx concentration, CHO cells added and, after 24 hrs growth, scored for normal or clustered morphology. The highest sera dilution completely preventing CHO cell clustering was recorded and compared versus purified control 1B7 antibody. This assay resulted in no statistically significant differences between groups on titre per μg antibody basis. Based on this assay, there is no evidence for a loss in antibody efficacy as a result of injection site (subcutaneous vs. IV) or formulation (Table 2). Western blot analysis was used to demonstrate the absence of gross physical changes in serum antibody due to formulation and administration route, such as formation of insoluble or disulfide bonded aggregates (data not shown). This *in vivo* data is consistent with our *in vitro* observations, that the protein within the dispersion shows no detectable loss of native size or activity during processing or *in vivo* administration.

Conclusions

Nanocluster dispersions allow monoclonal antibody formulation at high concentration and low viscosity, with no detectable loss in antibody size or activity *in vitro* or *in vivo* and similar pharmacokinetics when administered subcutaneously to mice. Highly concentrated ~190 mg/ml aqueous-based dispersions of a therapeutically relevant antibody, 1B7[37], were formed from stable, submicron protein particles containing a 1:1 weight ratio of trehalose in an aqueous buffer with multiple crowding agents, including trehalose, PEG and NMP. These particles were produced by rapid freezing in a dosage vial using SWIFT to minimize protein denaturation and aggregation, followed by lyophilization. A nanocluster dispersion was formed in the aqueous-based solvent near 1B7's pI by adding pharmaceutically acceptable crowding agents, PEG300 and NMP, along with the trehalose from the dry powder.

NIH-PA Author Manuscript

NIH-PA Author Manuscript

NIH-PA Author Manuscript

Additional analyses, ELISA, DLS and SDS-PAGE, indicate that the protein rapidly recovers a fully active monomeric form upon dilution of the dispersion with PBS. The apparent viscosity of the 190 mg/ml IgG dispersion with NMP and PEG through a 25 g 1.5″ needle was only 24 cP, reflecting the low initial solution viscosity and the low intrinsic viscosity. The measured *in vivo* distribution and elimination half-lives were similar for control solution and dispersion formulations administered at similar doses. The time to peak serum concentration (t_{max}) was delayed for the subcutaneous injections, consistent with the expected slower diffusion kinetics from this injection site. Remarkably, analysis of terminal serum samples was unable to detect a loss in 1B7 activity over the 14-day study period. This formulation strategy, in which crowding agents drive formation and stabilization of protein nanoclusters, has been shown to be applicable for both monoclonal and polyclonal antibodies. In this work, we demonstrate formulation with multiple crowding agents, which will provide flexibility in formulating additional therapeutic proteins. The ability to form stable, highly concentrated dispersions of a protein therapeutic with low viscosities and favorable bioavailability will increase the potential use of subcutaneous injection, possibly for treatment of many chronic diseases.

Supplementary Material

Refer to Web version on PubMed Central for supplementary material.

Acknowledgments

This work was supported by grants from the NIH (GM095638, JAM), the Packard Foundation (2005-098, JAM) and the McMakin family (JAM) as well as the Welch Foundation (F-1319, KPJ; F-1696, TMT), National Science Foundation (NSFSTC-CHE-9876674, KPJ; CBET-0968038, KPJ; CBET-1065357, TMT) and the Portuguese Foundation for Science and Technology (PTDC/EQU-EQU/104318/2008, MAR). We thank Dr. Jamie Sutherland for assistance with purification of the 1B7 antibody and Jamye O'Neal for assistance with *in vivo* procedures.

Abbreviations

DLS	dynamic light scattering
IgG	immunoglobulin
NMP	n-methyl-2-pyrrolidone
PEG	poly-ethylene glycol
pI	isoelectric point
PTx	pertussis toxin
SFD	spray freeze drying
SWIFT	spiral-wound in-situ freezing technique

References

1. Reichert JM, Rosensweig CJ, Faden LB, Dewitz MC. Monoclonal antibody successes in the clinic. Nat Biotechnol. 2005; 23(9):1073–1078. [PubMed: 16151394]
2. Nelson AL, Dhimolea E, Reichert JM. Development trends for human monoclonal antibody therapeutics. Nat Rev Drug Disc. 2010; 9:767–774.
3. Trevino SR, Scholtz JM, Pace CN. Measuring and increasing protein solubility. J Pharm Sci. 2008; 97(10):4155–4166. [PubMed: 18240286]
4. Chennamsetty N, Voynov V, Kayser V, Helk B, Trout BL. Design of therapeutic proteins with enhanced stability. PNAS. 2009; 106(29):11937–11942. [PubMed: 19571001]

NIH-PA Author Manuscript

NIH-PA Author Manuscript

NIH-PA Author Manuscript

5. Maynard JA, Maassen CB, Leppla SH, Brasky K, Patterson JL, Iverson BL, Georgiou G. Protection against anthrax toxin by recombinant antibody fragments correlates with antigen affinity. Nat Biotechnol. 2002; 20(6):597–601. [PubMed: 12042864]
6. Frokjaer S, Otzen DE. Protein Drug Stability: A Formulation Challenge. Nat Rev Drug Discovery. 2005; 4:298–306.
7. Yang MX, Shenoy B, Disttler M, Patel R, McGrath M, Pechenov S, Margolin AL. Crystalline monoclonal antibodies for subcutaneous delivery. PNAS. 2003; 100(12):6934–6939. [PubMed: 12782786]
8. Anonymous. RITUXAN® (Rituximab) full prescribing information. Genentech, Inc.; 2010.
9. Shire SJ, Shahrokh Z, Liu J. Challenges in the Development of High Protein Concentration Formulations. J Pharm Sci. 2004; 93(6):1390–1402. [PubMed: 15124199]
10. Dani B, Platz R, Tzannis ST. High Concentration Formulation Feasibility of Human Immunoglubulin G for Subcutaneous Administration. J Pharm Sci. 2007; 96(6):1504–1517. [PubMed: 17387698]
11. Neal BL, Asthagiri D, Lenhoff AM. Molecular Origins of Osmotic Second Virial Coefficients of Proteins. Biophys J. 1998; 75:2469–2477. [PubMed: 9788942]
12. Chi EY, Krishnan S, Kendrick BS, Chang BS, Carpenter JF, Randolph TW. Roles of conformational stability and colloidal stability in the aggregation of recombinant human granulocyte colony-stimulating factor. Protein Science. 2003; 12:903–913. [PubMed: 12717013]
13. Harn N, Allan C, Oliver C, Middaugh CR. Highly Concentrated Monoclonal Antibody Solutions: Direct Analysis of Physical Structure and Thermal Stability. J Pharm Sci. 2007; 96(3):532–546. [PubMed: 17083094]
14. Young TM, Roberts CJ. Structure and thermodynamics of colloidal protein cluster formation: Comparison of square-well and simple dipolar models. J Chem Phys. 2009; 131:125104. [PubMed: 19791922]
15. Liu J, Nguyen MDH, Andya JD, Shire SJ. Reversible Self-Association Increases the Viscosity of a Concentrated Monoclonal Antibody in Aqueous Solution. J Pharm Sci. 2005; 94(9):1928–1940. [PubMed: 16052543]
16. Sear RP. Interactions in protein solutions. Current Opinion in Colloid & Interface Science. 2006; 11:35–39.
17. Curtis RA, Prausnitz JM, Blanch HW. Protein-Protein and Protein-Salt Interactions in Aqueous Protein Solutions Containing Concentrated Electrolytes. Biotechnology and Bioengineering. 1998; 57(1):11–21. [PubMed: 10099173]
18. Johnston KP, Maynard JA, Truskett TM, Borwankar A, Miller MA, Wilson B, Dinin A, Khan T, Kaczorowski KJ. Concentrated dispersions of equilibrium protein nanoclusters that reversibly dissociate into active monomers. ACS Nano. 2012 in press.
19. Scherer TM, Liu J, Shire SJ, Minton AP. Intermolecular Interactions of IgG1 Monoclonal Antibodies at High Concentrations Characterized by Light Scattering. J Phys Chem B. 2010; 114:12948–12957. [PubMed: 20849134]
20. Kendrick BS, Carpenter JF, Cleland JL, Randolph TW. A transient expansion of the native state precedes aggregation of recombinant human interferon-γ. PNAS. 1998; 95:14142–14146. [PubMed: 9826667]
21. Wang W, Nema S, Teagarden D. Protein aggregation-Pathways and influencing factors. Int J Pharm. 2010; 390(2):89–99. [PubMed: 20188160]
22. Miller MA, Engstrom JD, Ludher BS, Johnston KP. Low Viscosity Highly Concentrated Injectable Nonaqueous Suspensions of Lysozyme Microparticles. Langmuir. 2010; 26(2):1067–1074. [PubMed: 19803503]
23. Defelippis, MR.; Akers, MJ. Peptides and Proteins as Parenteral Suspensions: an Overview of Design, Development, and Manufacturing Considerations. In: Frokjaer, S.; Hovgaard, L., editors. Pharmaceutical Formulation Development of Peptides and Proteins. Taylor & Francis Limited; Philadelphia: 2000. p. 113-143.
24. Shenoy B, Wang Y, Shan W, Margolin AL. Stability of Crystalline Proteins. Biotechnology and Bioengineering. 2001; 73(5):358–369. [PubMed: 11320506]

NIH-PA Author Manuscript NIH-PA Author Manuscript NIH-PA Author Manuscript

25. Foster TP, Moseley WM, Caputo JF, Alaniz GR, Leatherman MW, Yu X, Claflin WH, Reeves DR, Cleary DL, Zantello MR, Krabill LF, Wiest JR. Sustained elevated serum somatotropin concentrations in Holstein steers following subcutaneous delivery of a growth hormone releasing factor analog dispersed in water, oil or microspheres. J Controlled Release. 1997; 47:91–99.
26. Putney SD, Burke PA. Improving protien therapeutics with sustained-release formulations. Nature Biotechnology. 1998; 16:153–157.
27. Fu K, Klibanov AM, Langer R. Protein stability in controlled-release systems. Nature Biotechnology. 2000; 18:24–25.
28. Tae G, Kornfield JA, Hubbell JA. Sustained release of human growth hormone from in situ forming hydrogels using self-assembly of fluoroalkyl-ended poly(ethylene glycol). Biomaterials. 2005; 26(25):5259–5266. [PubMed: 15792553]
29. Mok H, Park TG. Water-free microencapsulation of proteins within PLGA microparticles by spray drying using PEG-assisted protein solubilization technique in organic solvent. Eur J Pharm Biopharm. 2008; 70(1):137–144. [PubMed: 18515053]
30. Zhu G, Mallery SR, Schwendeman SP. Stabilization of proteins encapsulated in injectable poly(lactide-co-glycolide). Nature Biotechnology. 2000; 18:52–57.
31. Gombotz WR, Pettit DK. Biodegradable Polymers for Protein and Peptide Drug Delivery. Bioconjugate Chem. 1995; 6(4):332–351.
32. Ye M, Kim S, Park K. Issues in long-term protein delivery using biodegradable microparticles. J Controlled Release. 2010; 146(2):241–260.
33. Singh M, Li X-M, McGee JP, Zamb T, Koff W, Wang CY, O'Hagan DT. Controlled release microparticles as a single dose hepatitis B vaccine: evaluation of immunogenicity in mice. Vaccine. 1997; 15(5):475–481. [PubMed: 9160514]
34. Cheung MS, Klimov D, Thirumalai D. Molecular crowding enhances native state stability and refolding rates of globular proteins. PNAS. 2005; 102(13):4753–4758. [PubMed: 15781864]
35. Shen VK, Cheung JK, Errington JR, Truskett TM. Insights into Crowding Effects on Protein Stability from Coarse-Grained Model. Journal of Biomechanical Engineering. 2009; 131:071002. (071007pg). [PubMed: 19640127]
36. Sato H, Sato Y. Protective activities in mice of monoclonal antibodies against pertussis toxin. Infect Immun. 1990; 58(10):3369–3374. [PubMed: 1698179]
37. Sutherland JN, Maynard JA. Characterization of a key neutralizing epitope on pertussis toxin recognized by the monoclonal antibody 1B7. Biochemistry. 2009; 48(50):11982–11993. [PubMed: 19899804]
38. Strickley RG. Solubilizing Excipients in Oral and Injectable Formulations. Pharm Res. 2004; 21(2):201–230. [PubMed: 15032302]
39. Ryoo W, Webber SE, Johnston KP. Water-in-Carbon Dioxide Microemulsions with Methylated Branched Hydrocarbon Surfactants. Ind Eng Chem Res. 2003; 42:6348–6358.
40. Sutherland JN, Chang C, Yoder SM, Rock MT, Maynard JA. Antibodies recognizing protective pertussis toxin epitopes are preferentially elicited by natural infection versus acellular immunization. Clin Vaccine Immunol. 2011; 18(6):954–962. [PubMed: 21508166]
41. Gillenius P, Jaatmaa E, Askelof P, Granstrom M, Tiru M. The standardization of an assay for pertussis toxin and antitoxin in microplate culture of Chinese hamster ovary cells. J Biol Stand. 1985; 13(1):61–66. [PubMed: 4039324]
42. Carpenter, JF.; Chang, BS.; Garzon-Rodrigues, W.; Randolph, TW. Rational design of stable lyophilized protein formulations: theory and practice. In: Carpenter, JF.; Manning, MC., editors. Pharmaceutical Biotechnology 13 Rational Design of Stable Protein Formulations. Kluwer; New York: 2002. p. 109-133.
43. Engstrom JD, Simpson DT, Cloonan C, Lai ES, Williams RO III, Kitto GB, Johnston KP. Stable high surface area lactate dehydrogenase particles produced by spray freezing into liquid nitrogen. European Journal of Pharmaceutics and Biopharmaceutics. 2007; 65:163–174. [PubMed: 17027245]
44. Chen B, Bautista R, Yu K, Zapata GA, Mulkerrin MG, Chamow SM. Influence of Histidine on the Stability and Physical Properties of a Fully Human Antibody in Aqueous and Solid Forms. Pharm Res. 2003; 20(12):1952–1960. [PubMed: 14725359]

NIH-PA Author Manuscript

NIH-PA Author Manuscript

NIH-PA Author Manuscript

45. Engstrom JD, Lai ES, Ludher BS, Chen B, Milner TE, Williams RO III, Kitto GB, Johnston KP. Formation of Stable Submicron Protein Particles by Thin Film Freezing. Pharm Res. 2008; 25(6): 1334–1346. [PubMed: 18286357]
46. Souillac PO, Middaugh CR, Rytting JH. Investigation of protein/carbohydrate interactions in the dried state. 2. Diffuse reflectance FTIR studies. Int J Pharm. 2002; 235:207–218. [PubMed: 11879755]
47. Carpenter, JF.; Chang, BS.; Randolph, TW. Physical Damage to Proteins During Freezing, Drying and Rehydration. In: Costantino, HR.; Pikal, MJ., editors. Lyophilization of Biopharmaceuticals. AAPS Press; 2005. p. 423-442.
48. Timasheff, SN. Stabilization of Protein Structure by Solvent Additives. In: Ahern, TJ.; Manning, MC., editors. Stability of Protein Pharmaceuticals: Part B. Springer; 1992. p. 265-285.
49. Carpenter, JF.; Izutsu, K-i; Randolph, TW. Freezing and drying induced perturbations of protein structure and mechanisms of protein protection by stabilizing additives. In: Rey, L.; May, JC., editors. Freeze Drying/Lyophilization of Pharmaceutical and Biological Products. Marcel Dekker, Inc.; New York: 2004. p. 147-186.
50. Allison SD, Chang BS, Randolph TW, Carpenter JF. Hydrogen Bonding between Sugar and Protein is Responsible for Inhibition of Dehydration-Induced Protein Unfolding. Archives of Biochemistry and Biophysics. 1999; 365(2):289–298. [PubMed: 10328824]
51. Webb SD, Cleland JL, Carpenter JF, Randolph TW. Effects of Annealing Lyophilized and Spray-Lyophilized Formulations of Recombinant Human Interferon-γ. J Pharm Sci. 2003; 92(4):715–729. [PubMed: 12661058]
52. Yu Z, Garcia AS, Johnston KP, Williams RO III. Spray freezing into liquid nitrogen for highly stable protein nanostructured microparticles. European Journal of Pharmaceutics and Biopharmaceutics. 2004; 58:529–537. [PubMed: 15451527]
53. Kueltzo LA, Wang W, Randolph TW, Carpenter JF. Effects of Solution Conditions, Processing Parameters and Container Materials on Aggregation of a Monoclonal Antibody during Freeze-Thawing. Journal of Pharmaceutical Sciences. 2008; 97(5)
54. Costantino HR, Firouzabadian L, Hogeland K, Wu CC, Beganski C, Carrasquillo KG, Cordova M, Griebenow K, Zale SE, Tracy MA. Protein spray-freeze drying. Effect of atomization conditions on particle size and stability. Pharm Res. 2000; 17:1374–1383. [PubMed: 11205730]
55. Engstrom JD, Simpson DT, Lai ES, Williams RO III, Johnston KP. Morphology of protein particles produced by spray freezing of concentrated solutions. European Journal of Pharmaceutics and Biopharmaceutics. 2007; 65:149–162. [PubMed: 17010582]
56. Maa Y-F, Prestrelski SJ. Biopharmaceutical powders: particle formation and formulation considerations. Current Pharmaceutical Biotechnology. 2000; 1:283–302. [PubMed: 11469385]
57. Kulkarni AM, Chatterjee AP, Schweizer KS, Zukoski CF. Effects of polyethylene glycol on protein interactions. J Chem Phys. 2000; 113(21):9863–9873.
58. Lu PJ, Zaccarelli E, Ciulla F, Schofield AB, Sciortino F, Weitz DA. Gelation of particles with short-range attraction. Nature. 2008; 453:499–503. [PubMed: 18497820]
59. Boncina M, Rescic J, Vlachy V. Solubility of Lysozyme in Polyethylene Glycol-Electrolyte Mixtures: The Depletion Interaction and Ion-Specific Effects. Biophys J. 2008; 95:1285–1294. [PubMed: 18441020]
60. Shulgin IL, Ruckenstein E. Preferential hydration and solubility of proteins in aqueous solutions of polyethylene glycol. Biophysical Chemistry. 2006; 120:188–198. [PubMed: 16377069]
61. Hiemenz, PC.; Rajagopalan, R. Principles of Colloid and Surface Chemistry. 3rd ed. Marcel Dekker, Inc.; New York: 1997. p. 650
62. Porcar L, Falus P, Chen W-R, Faraone A, Fratini E, Hong K, Baglioni P, Liu Y. Formation of the Dynamic Clusters in Concentrated Lyoszyme Protein Solutions. J Phys Chem Lett. 2010; 1:126–129.
63. Lafleche F, Durand D, Nicolai T. Association of Adhesive Spheres Formed by Hydrophobically End-Capped PEF. 1. Influence of the Presence of Single End-Capped PEO. Macromolecules. 2003; 36:1331–1340.

NIH-PA Author Manuscript

NIH-PA Author Manuscript

NIH-PA Author Manuscript

64. Kanai S, Liu J, Patapoff TW, Shire SJ. Reversible Self-Association of a Concentrated Monoclonal Antibody Solution Mediated by Fab-Fab Interaction That Impacts Solution Viscosity. J Pharm Sci. 2008; 97(10):4219–4227. [PubMed: 18240303]

65. Gabrielson JP, Brader ML, Pekar AH, Mathis KB, Winter G, Carpenter JF, Randolph TW. Quantitation of Aggregate Levels in a Recombinant Humanized Monoclonal Antibody Formulation by Size-Exclusion Chromatography, Asymmetrical Flow Field Flow Fractionation, and Sedimentation Velocity. J Pharm Sci. 2007; 96(2):268–279. [PubMed: 17080424]

66. Saluja A, Kalonia DS. Nature and consequences of protein-protein interactions in high protein concentration solutions. Int J Pharm. 2008; 358:1–15. [PubMed: 18485634]

67. Maas C, Hermeling S, Bouma B, Jiskoot W, Gebbink M. A role for protein misfolding in immunogenicity of biopharmaceuticals. J Biol Chem. 2007; 282(4):2229–2236. [PubMed: 17135263]

68. Pincus DL, Thirumalai D. Crowding Effects on the Mechanical Stability and Unfolding Pathways of Ubiquitin. J Phys Chem B. 2009; 113:359–368. [PubMed: 19072020]

69. Desai UR, Klibanov AM. Assessing the Structural Integrity of a Lyophilized Protein in Organic Solvents. J Am Chem Soc. 1995; 117:3940–3945.

70. Roberts CJ, Debenedetti PG. Engineering Pharmaceutical Stability with Amorphous Solids. AIChE Journal. 2002; 48(6):1140–1144.

71. Krishnan S, Chi EY, Webb JN, Chang BS, Shan D, Goldenberg M, Manning MC, Randolph TW, Carpenter JF. Aggregation of Granulocyte Colony Stimulating Factor under Physiological Conditions: Characterization and Thermodynamic Inhibition. Biochemistry. 2002; 41:6422–6431. [PubMed: 12009905]

72. Zhou H-X, Rivas G, Minton AP. Macromolecular Crowding and Confinement: biochemical, biophysical and potential physiological consequences. Annu Rev Biophys. 2008; 37:375–397. [PubMed: 18573087]

73. Wang W, Wang EQ, Balthasar JP. Monoclonal Antibody Pharmacokinetics and Pharmacodynamics. Clinical Pharmacology & Therapeutics. 2008; 84:548–558. [PubMed: 18784655]

74. Tabrizi MA, Tseng CM, Roskos LK. Elimination mechanisms of therapeutic monoclonal antibodies. Drug Discov Today. 2006; 11(1-2):81–88. [PubMed: 16478695]

NIH-PA Author Manuscript

NIH-PA Author Manuscript

NIH-PA Author Manuscript

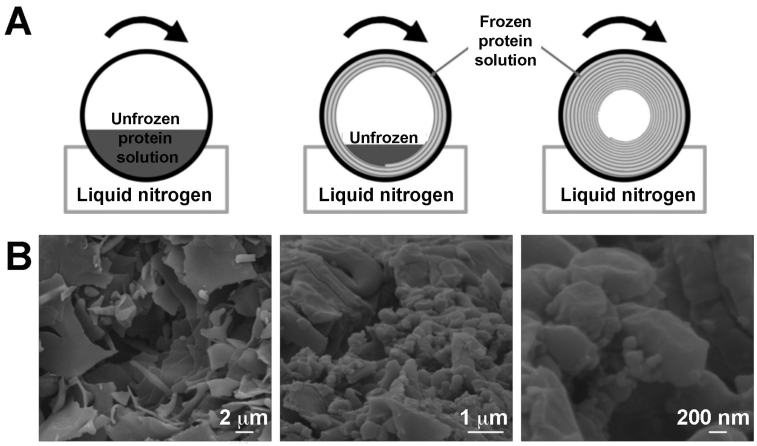

Figure 1. Schematic of SWIFT freezing process and dry powder SEM

A, The unfrozen protein solution in a cylindrical vial is placed on its side and rolled while exposed to liquid nitrogen. This causes a thin film of the protein solution to freeze on the inside edge of the vial followed by subsequent films towards the center of the vial resulting in a frozen annulus of protein solution which is placed in the lyophilizer to remove water. ***B,*** Morphology of SWIFT powder after lyophilization by SEM. Scale bars indicate 2 microns, 1 micron and 200 nm.

NIH-PA Author Manuscript

NIH-PA Author Manuscript

NIH-PA Author Manuscript

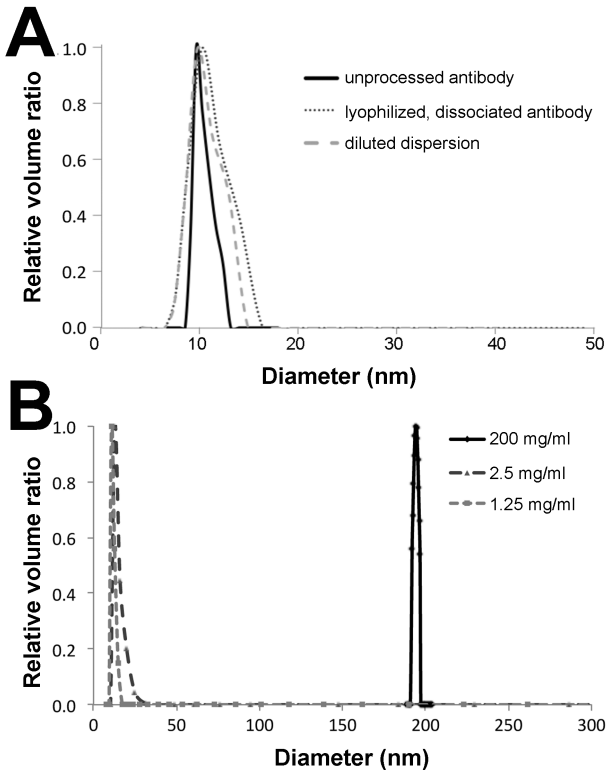

Figure 2. Size distribution of antibody particles

A. Comparison of unprocessed, lyophilized and dispersed 1B7 by DLS. All samples were diluted to 5 mg/ml in PBS. ***B.*** Effect of antibody concentration on particle size in dispersion buffer. At high concentration (200 mg/ml) in dispersion buffer, dynamic light scattering (DLS) detects only large particles of ~430 nm. Upon dilution below the threshold concentration for cluster formation in the dispersion buffer, concentrations of 2.5 and 1.25 mg/ml detect only particles of ~10 nm size, the expected size for monomeric IgG antibody. DLS data was analyzed by CONTIN.

NIH-PA Author Manuscript
NIH-PA Author Manuscript
NIH-PA Author Manuscript

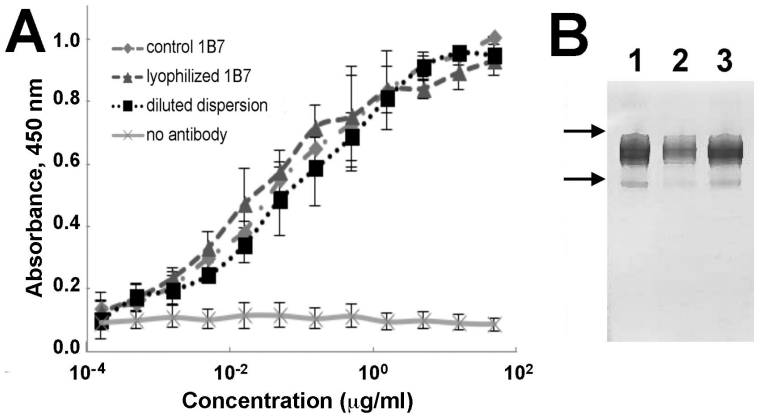

Figure 3. Characterization of antibody recovered from dispersion

A. Comparison of unprocessed, lyophilized and dispersed 1B7 by PTx ELISA to monitor antibody activity. ***B.*** SDS-PAGE gel comparing antibody 1B7 that is unprocessed, purified (lane 1), lyophilized, resuspended (lane 2) and a dispersion diluted from 200 to 1 mg/ml in PBS (lane 3). Arrows indicate the 175 and 140 kDa molecular weight markers.

NIH-PA Author Manuscript

NIH-PA Author Manuscript

NIH-PA Author Manuscript

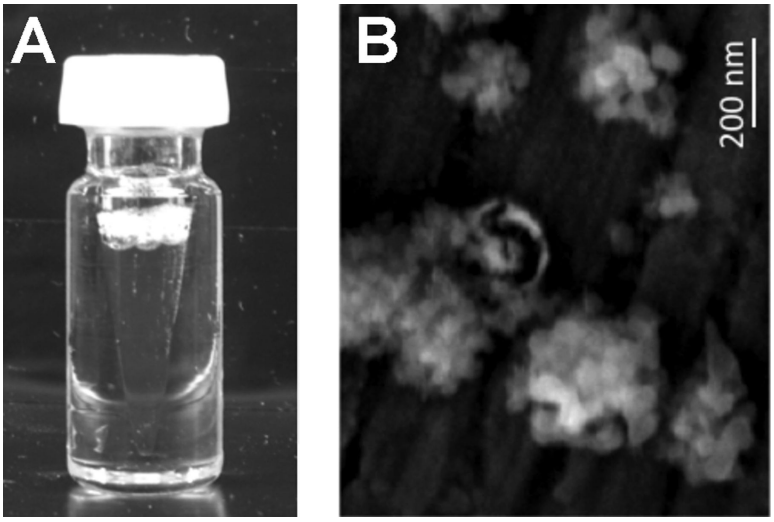

Figure 4. Visual appearance of dispersion

A. Digital image of suspended particles ***B.*** SEM image of antibody dispersion (200 mg/ml) when diluted to 100 mg/ml in the dispersion buffer, rapidly frozen and the water removed by lyophilization. Scale bar corresponds to 200 nm.

NIH-PA Author Manuscript

NIH-PA Author Manuscript

NIH-PA Author Manuscript

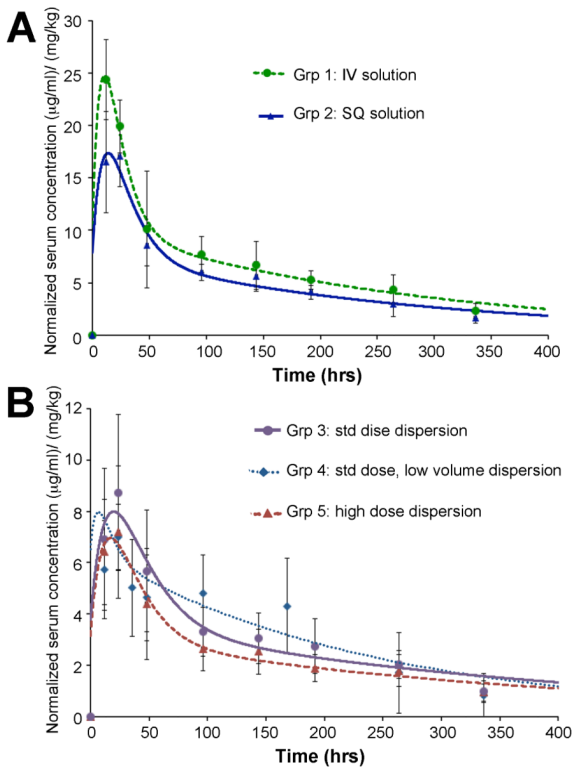

Figure 5. Serum concentrations of antibody 1B7 after delivery

The 1B7 antibody was formulated and administered to mice with the indicated volumes and doses. At the indicated times, tail vein samples were collected and the concentration of active antibody present measured by PTx ELISA, normalized by the administered dose and plotted. ***A***, Comparison of antibody 1B7 pharmacokinetics when delivered as a 100 µl solution. Group 1 mice received an IV administration at 5.6 mg/kg, while Group 2 mice received a subcutaneous delivery at 5.6 mg/kg. ***B,*** Comparison of 1B7 pharmacokinetics when delivered via subcutaneous dispersion with varying concentrations and injection volumes. Groups 3 mice received a standard dose as a diluted dispersion at 4.6 mg/kg in a 100 µl injection volume, Group 4 mice received a standard dose dispersion at 7.3 mg/kg in a 1 µl injection volume, while Group 5 mice received high-dose dispersion at 51.6 mg/kg dose in a 100 µl injection volume. Curve fits by spline fitting.

NIH-PA Author Manuscript

NIH-PA Author Manuscript

NIH-PA Author Manuscript

Table 1

Biophysical characterization of 1B7 dispersions

Dispersion buffer	Protein concentration	Solubility	Colloid diameter	Apparent viscosity	Relative binding activity*
20% NMP 10% PEG300	190 ± 10 mg/ml	>2.5 mg/ml	432 ± 16 nm	24 ± 7 cP	1.50 ± 0.32

*calculated as ($EC_{50, test}$/ $EC_{50, control}$)

NIH-PA Author Manuscript NIH-PA Author Manuscript NIH-PA Author Manuscript

Table 2

Pharmacokinetic parameters for antibody 1B7 formulations.

Group	N	Injection volume (μl)	Dose (mg/kg)	C_{max}/dose (μg/ml)/ (mg/kg)	$AUC_{0-\infty}$/ dose (μg·hr/ml)/(mg/ kg)	t_{max} (hours)	$t_{1/2,\alpha}$ (hours)	$t_{1/2,\beta}$ (hours)	Relative neutralization activity
1: IV solution *	6	100	5.6	25.5 ± 3.8	3582 ± 990	15.1 ± 0.7	45.7 ± 22.8	227.1 ± 24.9	2.3 ± 1.7
2: SQ solution *	4	100	5.6	18.8 ± 4.4	2699 ± 583	18.9 ± 3.1	43.4 ± 17.3	210.0 ± 17.4	1.0 ± 1.8
3: SQ diluted dispersion	5	100	4.6	9.1 ± 3.2	1790 ± 630	28.8 ± 12.0	54 ± 21 #	219 ± 25	0.4 ± 0.2
4: SQ dispersion, standard dose	5	1	7.3	7.3 ± 1.3	1345 ± 467	20.1 ± 3.2	49 ± 29 #	180± 16	0.5 ± 0.2
5: SQ dispersion, high dose	6	100	51.6	7.6 ± 2.6	1919 ± 566	20.2 ± 5.2	51 ± 23 #	250± 24	2.1 ± 1.0

* Data previously reported in (18)

$t_{1/2,\alpha}$ determined from 2 points for some mice